Pulse Schemes for Detection and Quantitative Estimation of Quaternary Carbons with Optional Proton Decoupling

Key words: NMR, ^{13}C NMR, quaternary carbons, proton-carbon couplings, quantitaive estimation, spectral editing, pulsed field gradients

Abstract

Four new pulse sequences which suppress primary, secondary and tertiary (CH_3, CH_2 and CH) carbons efficiently by creating multiple quantum coherences and then dephasing them by the application of pulsed field gradients without affecting the quaternary carbons are proposed for the detection of quaternary carbons. While two of the schemes incorporate proton decoupling during acquisition, the other two enable observation of long-range proton-carbon couplings, if any, due to the absence of proton decoupling during acquisition. The experimental demonstration for three samples, a hexapeptide [$(CH_3)_3$C-O-CO-Val-Val-Val-Aib-Val-Aib-OCH_3, where Aib is methyl-alanyl residue], cholesteryl acetate and friedelan-7-one are presented.

Introduction

Spectral editing methods, particularly for ^{13}C-NMR form a very important tool in spectral assignments. They have undergone a lot of evolution with time leading to techniques that are quicker and simpler to perform. While the multidimensional NMR methods are essential for complex systems with large number of interacting nuclei, the use of one-dimensional experiments continues to be important for relatively small molecules for quick and routine analyses of the spectra. As of now, a large number one-dimensional ^{13}C experiments are available for the spectral editing with their own advantages and disadvantages (1-16). Some of these techniques are designed for distinguishing and identifying carbons where the spectra provide signals with positive intensity for C and CH_2 carbons and with reversed intensity for CH and CH_3 carbons (1-7). The techniques such as the variants of INEPT (8-10) and DEPT (11-13) detect only protonated carbons with increased sensitivity due to polarization transfer. There are also efforts to completely separate primary, secondary, tertiary and quaternary carbons (14-15). Recently, the report of a sequence that detects only quaternary carbons suppressing all protonated carbon signals has been published (17). Here the suppression of the protonated carbon signals is achieved using proton decoupling and pulsed field gradients. In the present paper, four new pulse schemes for the detection of quaternary carbons are reported. Two of these schemes enable observation of long-range proton-carbon couplings, if any, due to the absence of proton decoupling. Another advantage of not using proton decoupling is that the possible temperature changes arising from the decoupling power are avoided.

Results and Discussion

Pulse techniques proposed and used for the detection and quantitative estimation of quaternary carbons with or without long-range proton couplings are shown in Figure 1. All the sequences are similar with difference of presence or absence of proton decoupling during relaxation and/or acquisition periods. In all these schemes CH_3, CH_2 and CH carbons are suppressed, efficiently by creating their multiple quantum coherences and then dephasing using pulsed field gradients. The quaternary carbons pass through unaffected.

Figure 1a involves proton decoupling during relaxation as well as during acquisition and hence it provides quaternary carbon spectrum with maximum sensitivity due to decoupling and nOe effect. Figure 1b is an inverse gated decoupled sequence for obtaining quaternary carbons. This is same as 1a except that decoupling is switched off during relaxation. Hence this sequence provides quaternary carbons without nOe enhancement and hence it is useful for quantitative estimation. Figure 1c is same as 1a except that proton decoupling is switched off during relaxation as well as during acquisition. Due to the absence of decoupling during acquisition, it provides quaternary carbons with long-range proton couplings. However, the absence of decoupling even during relaxation reduces sensitivity because of the absence of nOe effect. Figure 1d is a gated decoupled sequence for obtaining quaternary carbons with long-range proton couplings. This is same as Figure 1a except that decoupling is absent during acquisition and hence it provides quaternary carbons with long-range proton couplings. The advantage of this sequence over 1c is the gain in sensitivity due to decoupling during relaxation.

Detection of quaternary carbons in the recently reported a pulse scheme (Figure 2) is based on decoupling during acquisition to suppress the signals coming from CH_2 carbons while suppressing other protonated carbons by dephasing using pulsed field gradients (17). The vector picture in Figure 2 represents the simplistic way of visualization of the evolution of magnetization components for C, CH, CH_2 and CH_3 carbons at different point of times.

The pulse schemes presented in Figure 1 are similar to the scheme in Figure 2 till the end of the 2τ period. The difference is in the later part of the sequences wherein, at the end delay 2τ, an additional proton 90x pulse is incorporated in the new schemes. The evolution of the magnetization in Figure 1a for C, CH, CH_2 and CH_3 carbons is briefly explained below by the product operator formalism. I and S refer to ^{1}H and ^{13}C spins, respectively (18). Since all the four sequences of Figure 1 are similar, the explanation for Figure 1a is applicable to others as well. The phases of all the pulses are kept constant along x. Gradient pulse pair g_1:g_1 is used to remove the artifacts that might arise due to 180^o pulse imperfections and the gradient pulse g_2 is used for dephasing the multiple quantum coherences involving all the protonated carbons.

For quaternary carbons, the first 90^o_x carbon pulse creates transverse magnetization ($-I_y$). At the end of the delay period, 2τ, an echo is formed. This transverse magnetization is converted into S_z magnetization by the second carbon 90^o_x pulses which does not get affected due to the dephasing gradient pulse, $g_{2.}$ Finally, the last 90^o_x carbon pulse converts the z-magnetization into observable transverse magnetization.

For CH carbons, the first 90^o_x carbon pulse creates transverse carbon magnetization which evolves under the influence of the one bond coupling to proton, for a period 2τ. When the delay 2τ is set $1/2J_{CH}$, antiphase magnetization ($2I_zS_x$) is created. This antiphase magnetization gets converted into multiple quantum coherence ($-2I_yS_x$) with the subsequent carbon and proton 90^o_x pulses. The gradient pulse g_2 dephases these multiple quantum coherences, and thus the signals from CH carbons are suppressed.

For CH_2 carbons, the carbon transverse magnetization created after the first 90^o_x pulse evolves under the influence of the coupling to two directly attached protons during the delay period, 2τ. At the end of the evolution for a period of $2\tau = 1/2J_{CH}$, doubly antiphase magnetization ($-4I_{1z}I_{2z}S_y$) is created. This doubly antiphase magnetization gets converted into multiple quantum coherences ($-4I_{1y}I_{2y}S_z$) after the subsequent carbon and proton 90^o_x pulses. These coherences are dephased by the gradient pulse, g_2, and thus the signals arising from CH_2 are suppressed in this sequences. It may be noted that in the earlier scheme (Figure 2) the CH_2 carbons get converted into observable doubly antiphase transverse carbon magnetization. Therefore it was required to switch on the decoupler to make this antiphase magnetization unobservable (17).

Similarly, for CH_3 carbons triply antiphase magnetization of carbon ($8I_{1z}I_{2z}I_{3z}S_x$) is created at the end of the delay $2\tau=1/2J_{CH}$, due to the coupling of carbon to the three protons which gets converted into multiple quantum coherences ($-8I_{1y}I_{2y}I_{3y}S_x$) after the subsequent carbon and proton 90^o_x pulses. The gradient pulse g_2 dephases multiple quantum terms and hence the CH_3 carbons are also suppressed by this experiment.

Thus, in all the pulse schemes of Figure 1, protonated carbons are suppressed completely while passing only quaternary carbons. It is also clear that the need of proton decoupling is not necessary during acquisition. Hence it is possible to observe long-range proton-carbon couplings, if any when the proton decoupler is turned off during acquisition (Figure 1c and 1d). However, introduction of proton decoupling enables quaternary carbon detection with higher sensitivity due to narrow signals (Figure 1 a and 1b).

Experimental

Experiments using the new pulse schemes are demonstrated on a hexapeptide [$(CH_3)_3C$-O-CO-Val-Val-Val-Aib-Val-Aib-OCH_3, where Aib is methyl-alanyl residue], cholesteryl acetate and friedelan-7-one. All the spectra were recorded on a Bruker Avance 300 spectrometer equipped with z gradient accessory at 298 K temperature. The spectra were obtained on a 5 mm QNP probe with a spectral width of 15000, 32 K data points. The spectra were recorded with different number of scans varying from 16 to 200 for different sample and pulse schemes.

Figure 3, 4 and 5 show the ^{13}C spectra of the hexapeptide, up-field regions of cholesteryl acetate and friedelan-7-one, respectively, in $CDCl_3$ solvent. The structures the compounds are shown on top of the respective spectrum. Normal proton decoupled ^{13}C spectra are shown in (a**)**, Spectra shown in (b) are the respective SEFT sequence showing positive signals for quaternary carbons and negative signals for CH and CH_3 carbons (there are no CH_2 carbons in the hexapepte, Figure 3). Spectra (c) are obtained from the pulse scheme shown in Figure 2 for comparison. The spectra (d), (e), (f) and (g) are obtained from the pulse schemes shown in Figure 1a, 1b, 1c and 1d, respectively. The 2τ delay for the spectra (c) to (f) are set to 3.7, 4.2 and 4.2 ms for hexapeptide, cholesteryl acetate and friedelan-7-one, respectively.

It is clearly seen from the spectra (c) to (g) in Figures 3, 4 and 5 that the non-quaternary carbons are completely suppressed leaving behind only quaternary carbons. Quaternary carbons marked with asterisks in the structure of the peptide are observed in the spectra 3c to 3g between 50 and 85 ppm, while the others observed between 155 and 180 ppm are those coming from carbonyl carbons. It is seen from the spectra that the pulse schemes of Figure 1a and 1b provide sharp signals (spectra d and f) due proton decoupling and they are comparable with the spectra (c) obtained from the recently published scheme (Figure 2). Further due to the absence of decoupling during relaxation delay in Figure 1b, no enhancement of the signals occurs by the nOe effect and hence the spectra e obtained from this sequence can be used for quantitative estimation of the signals when recorded with sufficiently long relaxation delay.

As expected the quaternary signals in the spectra g and h are broad due to the large number long-range proton-carbon couplings. It is possible to observe well resolved multiplet structure for quaternary carbons from the systems with fewer number of long range coupled protons. Clearly, the sensitivity of the spectra (spectra g) obtained from scheme of Figure 1d is higher when compared to those obtained from Figure 1c (spectra e) due the gated decupling which enhances the signal intensity by nOe effect.

It is demonstrated that the sequence of Figure 2 is not critically dependent on the precise value of parameters such as the delay τ and the pulse widths (17). Similarly, we find that the sequences reported in this article are not critically dependent on the above parameters.

Conclusions

The spectral editing methods presented here for quaternary carbon detection are basically one-dimensional sequences with fewer number of RF pulses. It is noticed from the results of the proposed sequences that the quality of suppression of non-protonated carbons is extremely good. These, along with the tolerance of the pulse schemes to variations in the delay τ and the pulse widths appear to be important for routine applications. They also promise to play important role for the applications to systems with T_2 limiting cases as well as for low concentrated systems.

Acknowledgement

The authors are thankful to Professor. P. Balaram for graciously providing the peptide sample.

REFERENCES

1. Brown DW, Nakashima TT, Rabenstein DL. *J. Magn. Reson.*, 1981; **45**: 302-314.
2. Le Cocq C, Lallemand JY. *J. Chem. Commun.*, 1981; 150-152.
3. Patt S, Shoolery JN. *J. Magn. Reson.*, 1982; **46**: 535-539.
4. Madsen JC, Bildsoe H, Jakobsen H, Sorensen OW. *J. Magn. Reson.*, 1986; **67**: 243-257.
5. Torres AM, Nakashima TT, McClung RED. *J. Magn. Reson. Ser. A*, 1993; **101:** 285-294.
6. Homer J, Perry MC. *J. Chem. Soc. Chem. Commun.*, 1994; 373-374.
7. Homer J, Perry MC. *J. Chem. Soc. Perkin Trans.*, 1995; 533-536.
8. Morris GA, Freeman R. *J. Am. Chem. Soc.*, 1979; **101**: 760-762.
9. Burum DP, Ernst RR. *J. Magn. Reson.*, 1980; **39**: 163-168.
10. Sorensen OW, Ernst RR. *J. Magn. Reson.*, 1983; **51**: 477-489.
11. Bendall MR,. Doddrell DM, Pegg DT. *J. Am. Chem. Soc.*, 1981; **103**: 4603-4605.
12. Dodrell DM,. Pegg DT, Bendall MR. *J. Magn. Reson.*, 1982; **48**: 323-327.
13. Schenker KV, Philipsborn Wv. *J. Magn. Reson.*, 1986; **66**: 219-229.
14. Bildose H, Donstrup S, Jakobsen HJ, Sorensen OW. *J. Magn. Reson.*, 1983; **53**: 154-162.
15. Sorensen OW, Donstrup S, Bildose H, H. J. Jakobsen HJ. *J. Magn. Reson.*, 1983; **55**: 347-354.
16. Derome AE, In *Modern NMR Techniques for Chemistry Research*, Organic Chemistry Series, Volume 6, Baldwin JE (Ed), Pergamon Press, Oxford, 1987; 259-262.
17. Nagana Gowda GA, *Magn. Reson. Chem*., 2001; **39**: 581-585.
18. Sorensen OW, Eich GW, Levitt MH, Bodenhausen G, Ernst RR. *Prog. NMR Spectrosc.*, 1983; **16**: 163-192.

Figure captions

FIG. 1. Pulse schemes for quaternary carbons detection. Thin and thick filled bars represent 90° and 180° pulses, respectively. The default phase for the pulses is x. Gradient pulse pair g_1:g_1 remove the artifacts caused by the imperfect 180° pulses and the pulse, gradient g_2 is used for dephasing multiple quantum coherences involving protonated carbons. The duration and strength of the gradients used are g_1 = (1.0 ms, 5 G/cm); g_2 = (1.5 ms, 10 G/cm). (a) Pulse scheme for providing quaternary carbons with decoupling during relaxation as well as acquisition. (b) Inverse gated decoupled sequence for obtaining quaternary carbons for quantitative estimation (c) Pulse scheme for quaternary carbon detection with long-range proton couplings. Note that proton decoupler is off both during relaxtion and acquisition. (d) Gated decoupled pulse sequence for obtaining quaternary carbons with long-range proton couplings and enhanced sensitivity due to nOe effect.

FIG. 2. PFG-QCD pulse sequence for selective detection of quaternary carbons (17). Thin and thick filled bars represent 90° and 180° pulses, respectively. Gradient pulse pair g_1:g_1 is used to remove the artifacts caused by the imperfect 180° pulses

and the pulse, g_2 is a z-filtering gradient. The evolution of the product operators at different time points *a*, *b*, *c* and *d* is depicted by the vector pictures for C, CH, CH_2 and CH_3 carbons. The duration and strength of the gradients are g_1 = (1.0 ms, 5 G/cm); g_2 = (1.5 ms, 10 G/cm).

FIG. 3. ^{13}C spectra in $CDCl_3$ solvent of 20 mmol^{-1} hexapeptide with its structure shown at the top of the figure. (a) Normal proton decoupled ^{13}C spectrum; (b) SEFT spectrum showing positive signals for quaternary carbons and negative signals for CH and CH_3 carbons; (c) Spectrum obtained using the pulse sequence shown in Figure 2 with; (d) Spectrum obtained from pulse scheme of Figure 1a. Quaternary carbons seen between 50 and 85 ppm are observed re marked with asterisks in the structure. (e) Spectrum obtained from pulse schemes Figure 1b for quantitative estimation; (f) Spectrum obtained from pulse scheme of Figure 1c. Note the lines are broad due to long-range proton couplings (g) Spectrum obtained from pulse scheme of Figure 1d. Here the lines are broad due to long-range proton coupling but the intensities are much higher when compared to f due to the enhancement of the signals by decoupling during relaxation. The spectra c to g are obtained with a 2τ delay of 3.7 ms.

FIG. 4. Part of the ^{13}C spectra of 100 mg ml^{-1} cholesteryl acetate in $CDCl_3$ solvent recorded with 2τ delay of 4.2 ms. The pulse schemes used for obtaining the spectra (a) to (g) are same as those mentioned for Figure 3, respectively.

FIG. 5. Part of the ^{13}C spectra of 40 mg ml^{-1} friedelan-7-one in $CDCl_3$ solvent recorded with 2τ delay of 4.2 ms. The pulse schemes used for obtaining the spectra (a) to (g) are same as those mentioned for Figure 3, respectively. A dispersive signal around 41 ppm observed in g is an instrumental artifact.

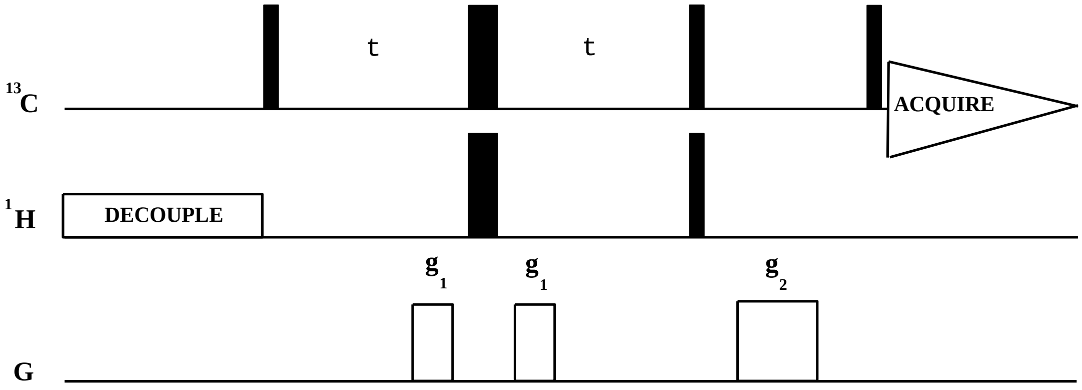
t
t
^{13}C
ACQUIRE
^{1}H
DECOUPLE
g_1
g_1
g_2
G

(d)

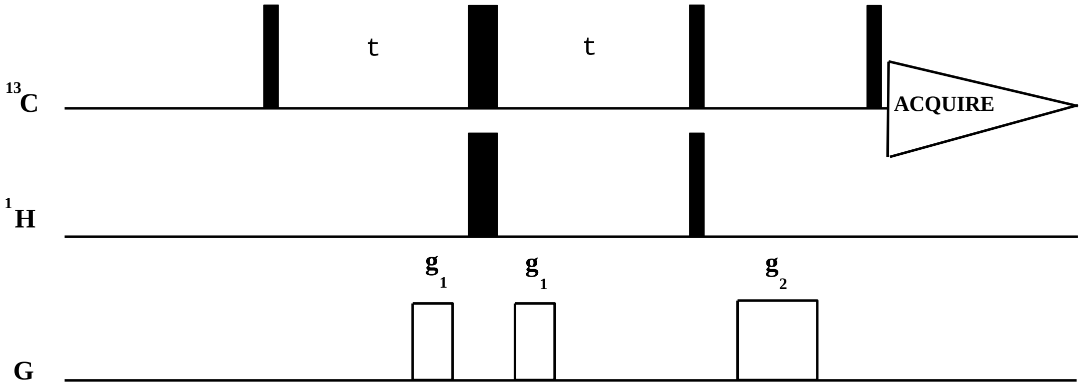
t
t
^{13}C
ACQUIRE
^{1}H
g_1
g_1
g_2
G

(c)

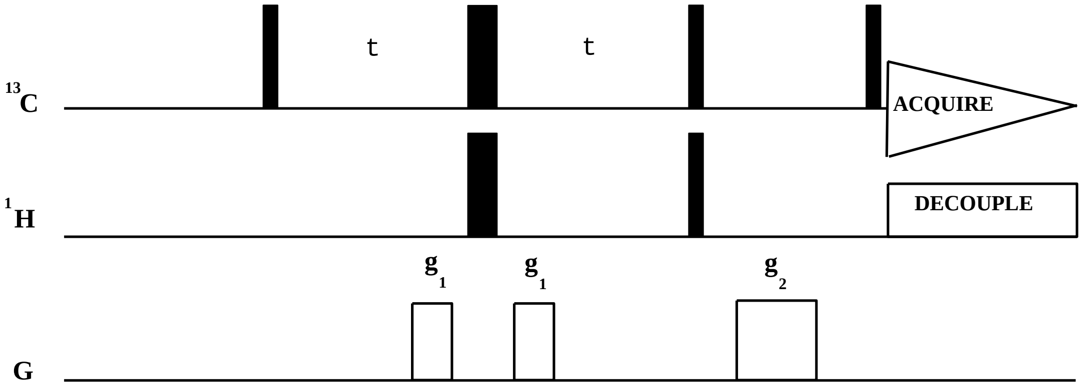
t
t
^{13}C
ACQUIRE
^{1}H
DECOUPLE
g_1
g_1
g_2
G

(b)

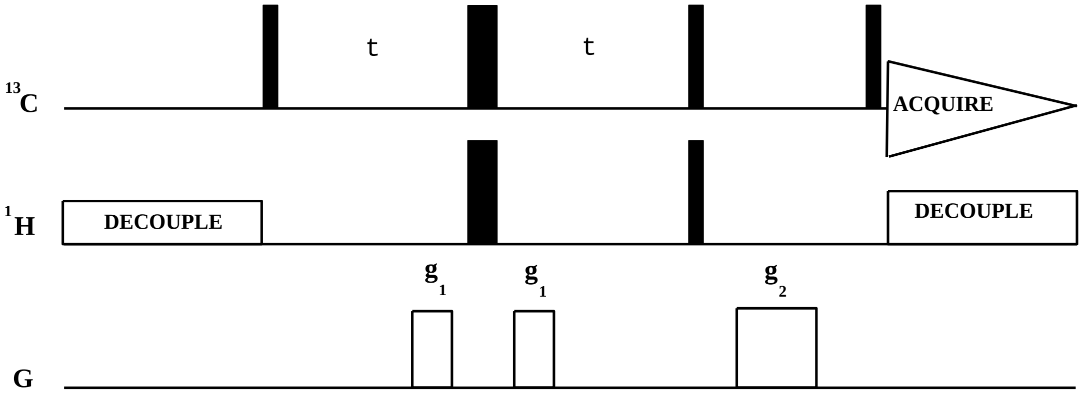
t
t
^{13}C
ACQUIRE
^{1}H
DECOUPLE
DECOUPLE
g_1
g_1
g_2
G

(a)